

---

---

MICROCRYSTALLINE, NANOCRYSTALLINE, POROUS,  
AND COMPOSITE SEMICONDUCTORS

---

---

## Raman Scattering in InSb Spherical Nanocrystals Ion-Synthesized in Silicon-Oxide Films

I. E. Tyschenko<sup>a,\*</sup>, V. A. Volodin<sup>a</sup>, and V. P. Popov<sup>a</sup>

<sup>a</sup> Rzhanov Institute of Semiconductor Physics, Siberian Branch, Russian Academy of Sciences, Novosibirsk, 630090 Russia

\*e-mail: [tys@isp.nsc.ru](mailto:tys@isp.nsc.ru)

Received October 25, 2018; revised November 5, 2018; accepted November 5, 2018

**Abstract**—The Raman spectra of SiO<sub>2</sub> films containing InSb spherical nanocrystals produced by ion-beam synthesis are studied. TO- and LO-like modes in the spectra of the InSb nanocrystals are detected at frequencies of 187 and 195 cm<sup>-1</sup>, respectively. The shift of these modes to high frequencies with respect to the corresponding frequencies in InSb bulk crystals is analyzed from the viewpoint of the influence of the quantum-confinement effect, strains in nanocrystals, the surface phonon frequency, and scattering at the frequency corresponding to stretched anion–cation modes at the surface of polar spherical nanocrystals. The position of the 195-cm<sup>-1</sup> mode corresponds to LO phonons in InSb nanocrystals hydrostatically compressed in the SiO<sub>2</sub> matrix at pressures of about 10 kbar. The 187-cm<sup>-1</sup> mode corresponds to resonance at the Fröhlich frequency.

DOI: 10.1134/S1063782619040262

### 1. INTRODUCTION

One of the aspects of the increased interest in studies of optical phonons localized in low-dimensional polar crystals is related to emerging opportunities for the use of such crystals in current silicon technology for the purpose of developing silicon-based optical communications. This will make it possible to increase the operating speed of microprocessors and to reduce heat generation by lowering the power consumption. As hybrid integrated circuits are designed and their active regions are reduced to a few nanometers, the role of optical phonons becomes more important. The localization of optical phonons in low-dimensional crystals can influence both the optical and electrical properties of these crystals. The localization of phonons influences also the Raman-scattering effect, which forms the basis of a method widely used for characterizing semiconductor structures in practice. In polar nanocrystals, along with the quantum-confinement effect, which is different for the longitudinal and transverse optical modes, the contribution of scattering at surface phonons appearing at the interface between the nanocrystal and the surrounding matrix and at the Fröhlich frequency increases [1]. For example, for large-size nanocrystals, a single surface mode, whose frequency is intermediate between the frequencies of the longitudinal optical (LO) and transverse optical (TO) modes, is often observed. The total contribution of the above-mentioned effects often gives rise to difficulties in interpreting the results and leads

to corresponding problems in characterizing nanocrystalline objects.

In InSb polar nanocrystals which offer a number of advantages over other direct-gap semiconductors, the optical-phonon spectrum depends to a large extent on both the properties of the matrix surrounding the nanocrystals and the method of their production. In the Raman spectra of InSb quantum dots (QDs) grown by molecular-beam epitaxy on InP substrates, two peaks were observed at frequencies of 181 and 192 cm<sup>-1</sup>. These peaks corresponded to the TO and LO phonon modes in the InSb matrix, but were shifted to higher frequencies, which was attributed to the presence of uniaxial and hydrostatic strains [2]. If the QDs were covered with an InP layer, only the high-frequency optical mode was observed, with a maximum at a frequency close to 195 cm<sup>-1</sup>. The absence of the TO mode was attributed to the shift of the optical-phonon frequency to higher frequencies because of residual strains and changing conditions of scattering in this case. In contrast, in the case of InSb nanocrystals synthesized in a silicon-oxide matrix during radio-frequency sputtering and subsequent fast thermal annealing at a temperature of 900°C for 1 min, a broad peak at the frequency 180 cm<sup>-1</sup> was dominant and assumed to be a superposition of the TO and LO phonon modes in the InSb matrix [3]. In the spectra of InSb nanocrystals synthesized in the SiO<sub>2</sub> matrix by magnetron-assisted sputtering, a low-frequency peak at 178 cm<sup>-1</sup> corresponding to the TO phonon mode in the InSb crystal matrix was dominant

as well [4]. A peak corresponding to the LO phonon mode was observed at a frequency of  $188\text{ cm}^{-1}$  as well, but its intensity was substantially lower. In [4], it was shown that the In–Sb bond length and the coordination number in nanocrystals at the InSb/SiO<sub>2</sub> interface differed from the corresponding quantities in the bulk. Specifically, the bond length in InSb QDs was  $0.02\text{ Å}$  shorter than the bond length in bulk InSb. This can make the quantum-confinement effect less pronounced.

Under the conditions of ion-beam synthesis, during which the formation and growth of InSb nuclei occur in the liquid phase, with subsequent crystallization upon cooling, In–Sb bonds also undergo strains [5]. These strains, as a rule, are hydrostatic and can be responsible for shifts in the optical-phonon frequencies. The straining of bonds can be accompanied also by redistribution of the static ion charge and by the corresponding change in the transverse electric field, which can also influence the scattering of light. A contribution to the optical-phonon spectrum can also be made by vibrations at the interface between the InSb nanocrystal and the surrounding matrix. In this context, the purpose of this study is to analyze the optical-phonon spectrum of InSb nanocrystals produced by ion-beam synthesis in a silicon-oxide matrix. The analysis is performed with consideration for the contributions of different mechanisms of scattering.

## 2. EXPERIMENTAL

The method of producing InSb nanocrystals in SiO<sub>2</sub> films is described in detail elsewhere [5]. With that in mind, the 300-nm-thick SiO<sub>2</sub> films thermally grown on Si substrates were implanted with In<sup>+</sup> and Sb<sup>+</sup> ions with an energy of 200 keV and a dose of  $8 \times 10^{15}\text{ cm}^{-2}$ . The parameters of irradiation allowed us to provide Gaussian profiles of the incorporated atoms, with a maximum at a depth of 110 nm from the SiO<sub>2</sub> film surface; the concentration of atoms in the profile was  $\sim 1.2 \times 10^{21}\text{ cm}^{-3}$ . In order to prevent the escape of In atoms from the SiO<sub>2</sub> films upon annealing, the SiO<sub>2</sub> films were coated with a single-crystal Si layer produced by the hydrogen-induced transfer technique. To do this, another Si wafer was first irradiated with H<sub>2</sub><sup>+</sup> ions with an energy of 140 keV and a dose of  $2.0 \times 10^{16}\text{ cm}^{-2}$ . Then the implanted sides of the first and second wafers were joined, and within the layer implanted with hydrogen ions, a Si layer was exfoliated and transferred from the second wafer to the first one. The irradiated samples were subsequently subjected to high-temperature annealing at a temperature of 500–1100°C in a nitrogen atmosphere for 30 min.

The Raman spectra were excited by argon laser radiation at a wavelength of  $\sim 514.5\text{ nm}$  at room temperature. The size of the spot of the probe beam was  $10\text{ }\mu\text{m}$ . The power of the laser beam on the sample sur-

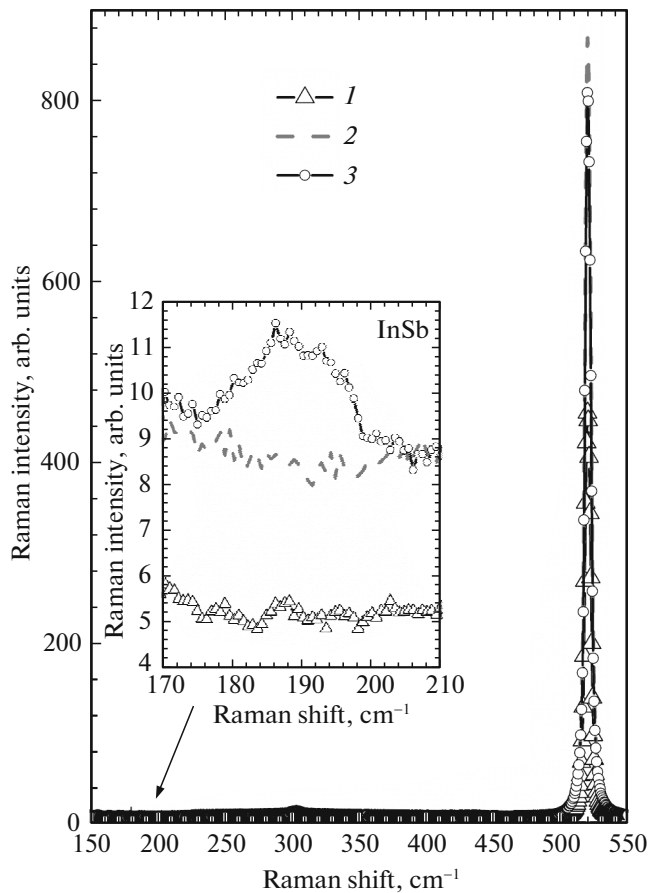
face was 2 mW. We used a T64000 (Horiba Jobin-Yvon) spectrometer with a triple monochromator; the spectral resolution was no worse than  $2\text{ cm}^{-1}$ . The detector was a silicon matrix of photodetectors cooled with liquid nitrogen. Studies were conducted in the backscattering layout of measurements; the polarization vector of incident radiation was directed along the  $\langle 011 \rangle$  crystallographic direction in silicon. The scattered light signal was detected for the  $\langle 01\bar{1} \rangle$  polarization. The forbidden geometric layout used in the measurements provided a means for maximally suppressing the scattered signal from the silicon substrate. To intensify the Raman signal from InSb nanocrystals, before the measurements, we removed the upper Si layer in a 25% solution of ammonium at a temperature of 40°C with continuous stirring.

## 3. RESULTS AND DISCUSSION

Figure 1 shows the Raman spectra recorded in the frequency range  $150\text{--}550\text{ cm}^{-1}$  for the single-crystal Si wafer and for the wafer coated with a SiO<sub>2</sub> layer immediately after implantation and after postimplantation annealing at a temperature of 800°C. For all of these samples, the principal Raman peak is at the frequency  $520.5\text{ cm}^{-1}$  and corresponds to the TO phonon mode in a single-crystal Si matrix. However, in the spectra of samples covered with a SiO<sub>2</sub> film implanted with In<sup>+</sup> and Sb<sup>+</sup> ions, the intensity of this peak is 1.8 times higher than that in the spectrum of the single-crystal Si wafer. Annealing at the temperature 800°C barely influences the intensity of this peak. In the three cases, the full width at half-maximum (FWHM) of the Raman peak is  $4.5\text{ cm}^{-1}$ . The results suggest that the SiO<sub>2</sub> film implanted with In<sup>+</sup> and Sb<sup>+</sup> ions is equally transparent before and after annealing. At the same time, the increase in the intensity of the Raman peak at the frequency  $520.5\text{ cm}^{-1}$  can be due to the fact that a SiO<sub>2</sub> layer with a suitable thickness acts as an antireflection coating.

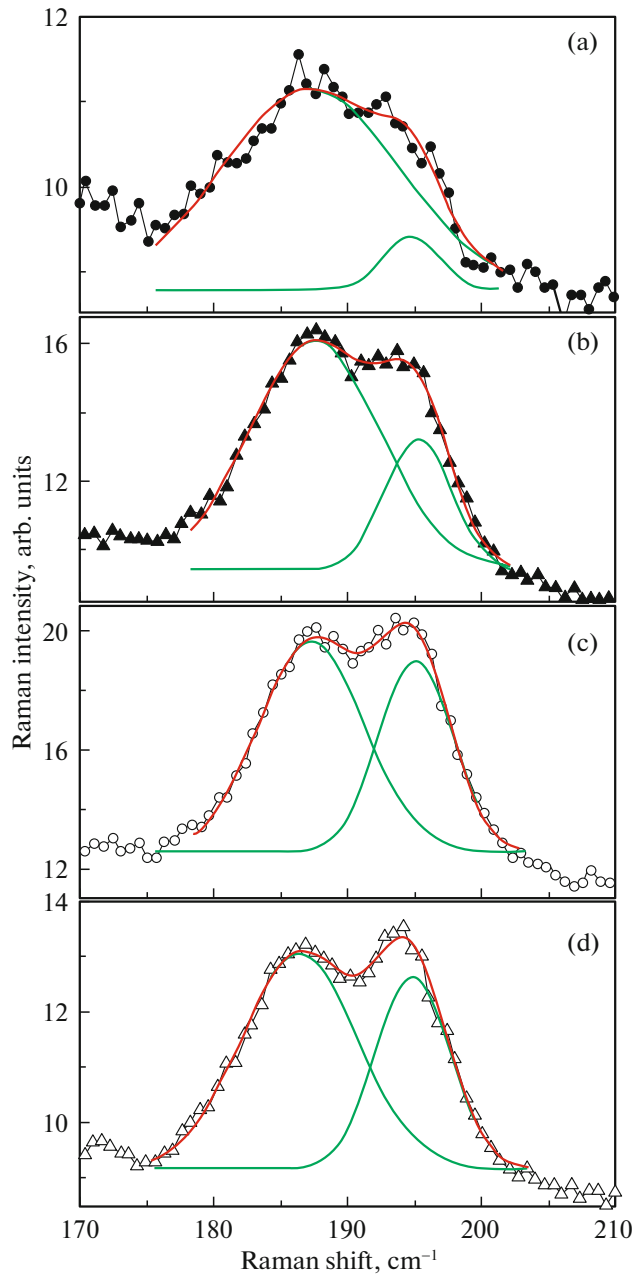
In the Raman spectrum shown in Fig. 1, we observe a  $300\text{ cm}^{-1}$  low-intensity peak, whose nature is associated with the doubled frequency of acoustic phonons in the single-crystal Si substrate. A detailed analysis of the Raman spectra shows that annealing of the samples at the temperature 800°C after implantation with In<sup>+</sup> and Sb<sup>+</sup> ions is accompanied by the appearance of a Raman band in the frequency range from  $\sim 180$  to  $\sim 200\text{ cm}^{-1}$  (see inset in Fig. 1). The nature of this band can be caused by scattering at the optical vibrations of In–Sb bonds in the crystalline InSb matrix.

Figure 2 shows the Raman spectra recorded in the frequency range  $170\text{--}210\text{ cm}^{-1}$  for implanted SiO<sub>2</sub> films after annealing at temperatures of 800, 900, 1000, and 1100°C. From Fig. 2, it can be seen that an increase in the annealing temperature from 800 to



**Fig. 1.** Raman spectra recorded in the frequency range 150–550  $\text{cm}^{-1}$  for (1) single-crystal silicon, (2, 3) silicon covered with a  $\text{SiO}_2$  layer (2) immediately after the implantation of  $\text{In}^+$  and  $\text{Sb}^+$  ions and (3) after implantation and annealing at a temperature of 800°C. The inset shows regions of the spectra in the frequency range 170–210  $\text{cm}^{-1}$ .

900°C yields an increase in the intensity of the Raman band. In addition, we can see well-pronounced peaks at frequencies of about 187 and 195  $\text{cm}^{-1}$ , which are close to the frequencies of the TO and LO optical phonon modes in the InSb matrix, but shifted to higher frequencies by 7.3 and 4.3  $\text{cm}^{-1}$ , respectively [6]. An increase in the annealing temperature to 1000°C results in a further increase in the intensity of the Raman peaks. As the annealing temperature is elevated to 1100°C, the Raman intensity at the above-indicated frequencies noticeably decreases. However, in this case, the peaks become sharper. To analyze the parameters of the observed Raman peaks, we decomposed the experimental spectra into two Gaussian components with maxima at 187 and 195  $\text{cm}^{-1}$ . The analysis shows that, in the spectra of the samples annealed at a temperature below 1000°C, the low-frequency TO-like mode is dominant. In this case, as the annealing temperature is elevated from 800 to 1000°C,



**Fig. 2.** Raman spectra recorded in the frequency range 170–210  $\text{cm}^{-1}$  for implanted  $\text{SiO}_2$  films after annealing at the temperatures (a) 800, (b) 900, (c) 1000, and (d) 1100°C.

the FWHM of this mode decreases from 13 to  $\sim 7$   $\text{cm}^{-1}$ . At annealing temperatures of 1000–1100°C, the intensities of the TO- and LO-like modes become comparable. It should be noted that the FWHM of the LO-like mode varies with temperature only slightly and corresponds to 4.5–5  $\text{cm}^{-1}$ .

The variations in the intensities of the Raman peaks with increasing annealing temperature correlate with variations in the density of nanocrystals formed

in the SiO<sub>2</sub> matrix during annealing [5]. Therefore, the Raman peaks observed at the frequencies 187 and 195 cm<sup>-1</sup> can be naturally attributed to the TO and LO phonon modes in InSb nanocrystals. A decrease in the splitting of the optical phonon is observed in parallel with the shift of the TO and LO modes in the spectra of InSb nanocrystals to higher frequencies with respect to the TO and LO modes in the spectrum of the single-crystal bulk material. In the experiments performed in this study, this splitting is 8 cm<sup>-1</sup>, whereas in the single-crystal InSb bulk, the splitting is 11 cm<sup>-1</sup>. It should be emphasized that the difference of 3 cm<sup>-1</sup> is independent of the annealing temperature; i.e., the difference is independent of the nanocrystal dimensions. The experimentally observed shifts of the TO and LO modes to higher frequencies are effective quantities dependent on a number of factors, such as the quantum-confinement effect, strains, and the state of the interface between the nanocrystal and the surrounding SiO<sub>2</sub> matrix. The contribution of each of these factors to the shift of the TO and LO phonon lines is estimated below.

To take into account the contribution of the quantum-confinement effect to the shift of the optical-phonon frequency in InSb nanocrystals, we calculated the Raman spectra in relation to the nanocrystal size in the context of the model of the spatial localization of phonons [7–9]. Because of an increase in the quasimomentum uncertainty, the spectrum of a phonon localized in a nanocrystal can be represented as a superposition of plane modes with the wave vector  $q$  in the vicinity of the wave vector  $q_0$  in an infinite crystal [9]. In this case, the wave function of a spatially confined phonon,  $\Psi(q_0, r)$ , is the product of the Bloch function  $\Phi(q_0, r)$ , which describes a phonon in an infinite crystal, and some envelope function  $W(r, L)$  with a characteristic size equal to that of the crystal  $L$ :

$$\Psi(q_0, r) = W(r, L)\Phi(q_0, r) = \Psi'(q_0, r)u(r). \quad (1)$$

Here  $\Phi(q_0, r) = u(r)\exp(iq_0r)$  is the phonon wave function in an infinite crystal,  $u(r)$  is a periodic function with a period equal to the InSb lattice period, and  $r$  is the coordinate in the lattice. In relation (1), we have

$$\Psi'(q_0, r) = W(r, L)\exp(iq_0r). \quad (2)$$

The function  $\Psi(q_0, r)$  can be written as the Fourier transform:

$$\Psi'(q_0, r) = \int C(q_0, q)\exp(iq_0r)d^3q, \quad (3)$$

where  $C(q_0, q)$  is the Fourier coefficient, which is the Fourier transform of the function  $\Psi'(q_0, r)$ . The probability that a phonon with the momentum  $\hbar q$  will be detected in this superposition of waves is  $|C(q, q_0)|^2$ . In the approximation of a spherical Brillouin zone for a

continuous mechanical medium, the intensity of the Raman signal can be expressed as

$$I(\omega) = \frac{1}{(2\pi)^3} \int \frac{|C(q, q_0)|^2 d^3q}{[\omega - \omega(q)]^2 + \left(\frac{\Gamma_0}{2}\right)^2}. \quad (4)$$

Here,  $\omega(q)$  is the phonon dispersion relation and  $\Gamma_0 = 8$  cm<sup>-1</sup> is the FWHM of a single phonon mode in the single-crystal InSb bulk [4], and  $|C(0, q)|^2$  is a decreasing function that describes the degree of phonon localization in the crystal. The function  $|C(0, q)|^2$  can be represented as [9]

$$|C(0, q)|^2 = \exp\left(\frac{-q^2 L^2}{8}\right). \quad (5)$$

Taking into account expression (5), we obtain the frequency dependence of the Raman intensity as

$$I(\omega) = \frac{1}{(2\pi)^3} \int \frac{\exp\left(\frac{-q^2 L^2}{8}\right) d^3q}{[\omega - \omega(q)]^2 + \left(\frac{\Gamma_0}{2}\right)^2}. \quad (6)$$

In (6), integration with respect to  $q$  is performed between the limits  $q = 0$  and  $q = q_1$ , where  $q_1 = \pi/a$  is the wave vector at the boundary of the Brillouin zone and  $a = 0.648$  nm is the lattice constant of InSb. The dispersion relation for phonons  $\omega(q)$  corresponds to the dispersion relation for a linear chain consisting of two kinds of atoms with the masses  $m_1$  and  $m_2$ . The expression for the dispersion of phonons,  $\omega(q)$ , was derived from the Lagrange equation for an infinite linear chain:

$$\omega_{1,2} = \frac{\beta}{m_1 m_2} \left[ (m_1 + m_2) + \sqrt{m_1^2 + m_2^2 + 2m_1 m_2 \cos(qa)} \right]. \quad (7)$$

Here  $m_1 = 114.8$  amu is the In atomic mass,  $m_2 = 121.7$  amu is the Sb atomic mass, and  $\beta$  is the coefficient of elasticity dependent on the vibrational-mode frequency as

$$\beta_{\text{LO,TO}} = \left(\frac{1}{m_1} + \frac{1}{m_2}\right) \frac{1}{2\omega_{\text{LO,TO}}^2}, \quad (8)$$

where  $\omega_{\text{LO}} = 190.7$  cm<sup>-1</sup> and  $\omega_{\text{TO}} = 179.7$  cm<sup>-1</sup> are, correspondingly, the frequencies of the LO and TO modes in the InSb single crystal [7].

The frequencies of the TO and LO modes were calculated as functions of the radius of the InSb spherical crystal. The results of the calculations are shown in Fig. 3. According to the results, for nanocrystals with a radius of <10 nm, the optical-phonon lines exhibit asymmetric broadening and a shift of the maxima to lower frequencies. For nanocrystals with a radius of >10 nm, the frequencies of the LO and TO modes are practically the same as those in the bulk single-crystal

InSb matrix. It should be emphasized that no influence of the nanocrystal size on the splitting of the optical phonon mode is detected. Irrespective of the nanocrystal size, the splitting is always  $11 \text{ cm}^{-1}$  and corresponds to the splitting in bulk single-crystal InSb. Thus, the calculations show that there is no confinement effect in the optical-phonon spectrum of InSb nanocrystals, whose dimensions are  $>10 \text{ nm}$ .

The effect of strains on the optical-phonon frequency can be taken into consideration on the basis of the dependences obtained in [7]. In [7], it was experimentally shown that the optical-phonon frequencies increased nearly linearly with increasing pressure  $P$ . In this case, the lattice constant changed almost proportionally to the applied pressure as well. The experimentally obtained dependences were approximated by the expressions

$$\begin{aligned}\omega_{\text{TO}} &= 179.7 + 5.01P - 0.10P^2 \\ &= 179.7 - 761(\Delta a/a),\end{aligned}\quad (9)$$

$$\begin{aligned}\omega_{\text{LO}} &= 190.7 + 5.11P - 0.31P^2 \\ &= 190.7 - 668(\Delta a/a),\end{aligned}\quad (10)$$

where the frequency  $\omega$  is expressed in  $\text{cm}^{-1}$  and the pressure  $P$  in GPa. The strain  $\Delta a/a$  can be estimated from the shift of the line at the highest frequency in the optical-phonon spectrum, i.e., from the LO phonon frequency  $\omega_{\text{LO}}$ . The point is that the LO phonon frequency is least distorted by other vibrations, whereas the observed shift of the TO mode can be distorted, for example, by scattering at surface phonons. From expression (10), it follows that the strain corresponding to the LO phonon frequency  $195 \text{ cm}^{-1}$  (Fig. 2) is  $-0.0064$ . In turn, this strain is bound to be attained at pressures of about 10 kbar [7]. According to expression (9), such a pressure corresponds to the TO phonon frequency  $\sim 184.5 \text{ cm}^{-1}$ , which is  $\sim 2.5 \text{ cm}^{-1}$  lower than the frequency observed experimentally.

As already noted above, the surface phonons at the interface between the InSb nanocrystal and the surrounding Si matrix can be one of the causes of the experimentally observed splitting of the optical phonon mode. In the experiments of this study, the nanocrystal diameter is comparable to the phonon correlation length. Therefore, we can naturally assume that there is a planar InSb/Si<sub>2</sub> interface. The lack of shifts of the low-frequency peak in the Raman spectrum can also be an argument for the inference about the lack of the size-dependent effect on the surface-phonon frequency. The condition for the existence of the surface mode can be written as

$$\epsilon_{\text{SiO}_2} + \epsilon_{\text{InSb}} = 0. \quad (11)$$

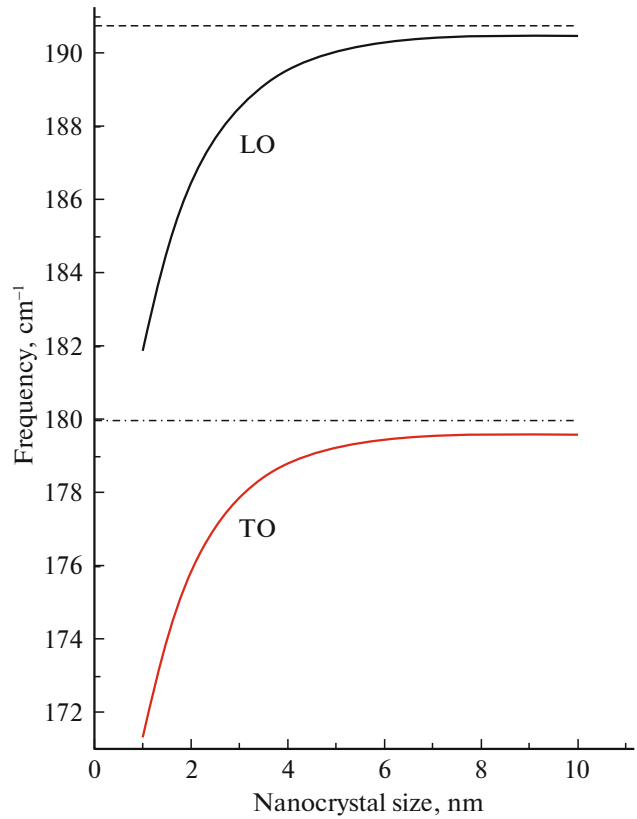


Fig. 3. TO and LO mode frequencies calculated in the context of the model of phonon spatial localization versus the radius of an InSb spherical nanocrystal.

Here,  $\epsilon_{\text{SiO}_2} = 3.9$  is the static permittivity of SiO<sub>2</sub> and  $\epsilon_{\text{InSb}}$  is the permittivity of the InSb polar crystal and depends on the frequency [10]:

$$\epsilon_{\text{InSb}}(\omega) = \epsilon_{\infty} \frac{\omega_{\text{LO}}^2 - \omega^2}{\omega_{\text{TO}}^2 - \omega^2}. \quad (12)$$

Upon the substitution of expression (12), expression (11) takes the form

$$\epsilon_{\text{SiO}_2} + \epsilon_{\infty} \frac{\omega_{\text{LO}}^2 - \omega^2}{\omega_{\text{TO}}^2 - \omega^2} = 0, \quad (13)$$

where  $\omega_{\text{LO}} = 195 \text{ cm}^{-1}$  is determined from the experiment (Fig. 2) and  $\epsilon_{\infty} = 15.9$ . With consideration for strains, the TO-like phonon frequency is  $184 \text{ cm}^{-1}$ . Substituting these values in (13), we determine the surface phonon frequency  $\omega = 192 \text{ cm}^{-1}$ . This value is  $5 \text{ cm}^{-1}$  larger than the experimentally observed TO-like phonon frequency. We can conceive that the experimentally observed low-frequency peak in the Raman spectrum is a superposition of the TO phonon mode and the surface phonon mode.

In the experiments performed in this study, the SiO<sub>2</sub> film contains InSb spherical crystals, whose dimensions are much smaller than the wavelength of

incident light. At the same time, the permittivities of InSb and SiO<sub>2</sub> are markedly different. In such media, it is possible to observe scattering at the Fröhlich frequency [11]. The Fröhlich resonance is observed at frequencies corresponding to stretched anion–cation modes at the surface of spherical nanocrystals and does not depend on the size of nanoparticles, at which scattering occurs [12]:

$$\omega_F = \left( \frac{\epsilon_\infty \omega_{LO}^2 + 2\epsilon_{SiO_2} \omega_{TO}^2}{\epsilon_\infty + 2\epsilon_{SiO_2}} \right)^{1/2}. \quad (14)$$

Substituting the permittivities of SiO<sub>2</sub> and InSb and the frequencies of the LO and TO modes in bulk single-crystal InSb in expression (14), we obtain the Fröhlich resonance frequency  $\omega_F = 187 \text{ cm}^{-1}$ . This frequency exactly coincides with the experimentally observed position of the low-frequency component in the Raman spectrum (Fig. 2). At a qualitative level, the temperature dependence of the intensity and width of the low-frequency peak in the Raman spectrum corresponds to the behavior of the Fröhlich mode as well. Specifically, as the annealing temperature is elevated and, consequently, the average nanocrystal dimensions are increased, the intensity of scattering at nanocrystals increases and, in parallel, the line width decreases. At the same time, since the Fröhlich resonance frequency depends on the frequencies of the TO and LO modes, it can also be shifted to higher frequencies in ion-synthesized strained nanocrystals. According to estimations with consideration for strains, the Fröhlich frequency  $\omega_F$  can be  $\sim 191 \text{ cm}^{-1}$ . In order to establish whether or not the nature of the observed peak is defined by resonance at the Fröhlich frequency, it is necessary to conduct additional studies by means of far-infrared absorption spectroscopy.

#### 4. CONCLUSIONS

The Raman spectra of SiO<sub>2</sub> films containing InSb spherical nanocrystals are studied. The nanocrystals are produced by ion-beam synthesis upon the implantation of SiO<sub>2</sub> films with In<sup>+</sup> and Sb<sup>+</sup> ions with an energy of 200 keV and a dose of  $8 \times 10^{15} \text{ cm}^{-2}$  followed by annealing at temperatures of 800–1100°C. The TO- and LO-like modes in the Raman spectra of InSb nanocrystals are detected at the frequencies 187 and 195 cm<sup>-1</sup>, respectively. The shifts of these TO- and LO-like modes with respect to their position in InSb bulk nanocrystals are, correspondingly, 7.3 and 4.3 cm<sup>-1</sup> and do not depend on the nanocrystal size. It is found that the LO–TO splitting of optical phonons is 8 cm<sup>-1</sup>. This value is 3 cm<sup>-1</sup> smaller than the splitting in the bulk crystal. An increase in the annealing temperature from 800 to 1000°C, which corresponds to an increase in the average InSb nanocrystal dimensions from  $\sim 10$  to  $\sim 20 \text{ nm}$  [5], results in a decrease in the width of the TO-like mode and an

increase in its intensity. The LO-like mode increases in intensity as well, but its width remains practically unchanged. The results obtained in the study are analyzed from the viewpoint of the quantum-confinement effect, strains in nanocrystals, optical-phonon frequency, and scattering at the frequency corresponding to stretched anion–cation modes at the surface of polar spherical nanocrystals. From the analysis, it is concluded that the 195 cm<sup>-1</sup> mode corresponds to LO phonons in InSb nanocrystals hydrostatically compressed in the SiO<sub>2</sub> matrix at pressures of about 10 kbar. The 187-cm<sup>-1</sup> mode corresponds to resonance at the Fröhlich frequency.

#### ACKNOWLEDGMENTS

The study was supported by the Ministry of Education and Science of the Russian Federation, project no. GZ 0306-2016-0004.

#### REFERENCES

1. M. I. Vasilevskiy, *Phys. Rev. B* **66**, 195326 (2002).
2. G. Armelles, T. Utzmeier, P. A. Postigo, F. Briones, J. C. Ferrer, P. Peirò, and A. Comet, *J. Appl. Phys.* **81**, 6339 (1997).
3. B. Capoen, V. Q. Lam, S. Turrel, L. P. Vilcot, F. Beclin, Y. Jestin, and M. Bouazaoui, *J. Non-Cryst. Sol.* **351**, 1819 (2005).
4. D. Chen, C. Li, Z. Zhu, J. Fan, and S. Wei, *Phys. Rev. B* **72**, 075341 (2005).
5. I. E. Tyschenko, M. Voelskow, A. G. Cherkov, and V. P. Popov, *Semiconductors* **48**, 1228 (2014).
6. I. H. Campbell and P. M. Fauchet, *Solid State Commun.* **58**, 739 (1986).
7. K. Aoki, E. Anastassakis, and M. Cardona, *Phys. Rev. B* **30**, 681 (1984).
8. H. Richter, Z. P. Wang, and L. Ley, *Solid State Commun.* **39**, 625 (1981).
9. V. A. Volodin and V. A. Sachkov, *J. Exp. Theor. Phys.* **116**, 87 (2013).
10. P. Y. Yu and M. Cardona, *Fundamentals of Semiconductors. Physics and Materials Properties*, Ed. by H. E. Stanley and W. T. Rhodes (Springer, Heidelberg, Dordrecht, London, New York, 2010).
11. R. Ruppin and R. Englman, *Rep. Progr. Phys.* **33**, 149 (1970).
12. M. I. Vasilevskiy, A. G. Rolo, M. V. Artemyev, S. A. Filonovich, M. J. M. Gomes, and Yu. P. Rakovich, *Phys. Status Solidi B* **224**, 599 (2001).

*Translated by E. Smorgonskaya*